REVISTA BIO CIENCIAS
http://revistabiociencias.uan.edu.mx
https://doi.org/10.15741/revbio.12.e1878
ISSN 2007-3380

Original article / Artículo original

Synthesis of gold and silver nanoparticles anchored in graphene oxide

Síntesis de nanopartículas de oro y plata ancladas en óxido de grafeno

Del Real-Quiñonez, W.A. [1], *Lomelí-Rosales, D.A.* [2], *Ramírez-González, D.* [3], *Guevara-Martínez, S.J.* [4], *Escutia-Gutiérrez, R.* [5], *Del Río-Chávez, A. A.* [6], *Zamudio-Ojeda A.*[*1].

[1] *Departamento de Física, Centro Universitario de Ciencias Exactas e Ingenierías, Universidad de Guadalajara, Guadalajara, 44430, México.*
[2] *Departamento de Química, Centro Universitario de Ciencias Exactas e Ingenierías, Universidad de Guadalajara, Blvd. Marcelino García Barragán 1421, Guadalajara 44430, Jalisco, México.*
[3] *Posgrado Fis. Mat. CU Valles, Universidad de Guadalajara, 44430, México.*
[4] *Departamento de Farmacobiología, Centro Universitario de Ciencias Exactas e Ingenierías, Universidad de Guadalajara, Guadalajara, 44430, México.*
[5] *Departamento de Biología Molecular y Genómica, Centro Universitario de Ciencias de la Salud, Universidad de Guadalajara, Guadalajara, 44340, México.*
[6] *Laboratorio de Bromatología, Facultad de Agrobiología "Presidente Juárez", Universidad Michoacana de San Nicolás de Hidalgo, Paseo Lázaro Cárdenas, 2290, Uruapan, C.P. Uruapan, C.P. 60170, Uruapan, Michoacán, México.*

ABSTRACT

This study describes a series of experiments aimed at anchoring silver (AgNPs) and gold (AuNPs) nanoparticles onto graphene oxide (GO). In the first stage, the synthesis of colloidal nanoparticles was carried out using the Turkevich method, employing sodium citrate as a reducing and stabilizing agent. Subsequently, the nanoparticles were anchored to GO, which was synthesized using Hummers' method, involving the oxidation of graphite using potassium permanganate ($KMnO_4$), sodium nitrate ($NaNO_3$), and sulfuric acid ($H2SO_4$). Two methodologies were developed for anchoring: (1) mixing a solution of Au or Ag nanoparticles with graphene oxide, and (2) in situ synthesis of nanoparticles in a GO solution. The obtained samples were characterized using ultraviolet-visible spectroscopy (UV-Vis), scanning electron microscopy (SEM), high-resolution transmission electron microscopy (HRTEM), dynamic light scattering (DLS), and powder X-ray diffraction (XRD). The results indicate that both methods are effective for nanoparticle anchoring, resulting in homogeneous distributions and good structural properties. This study provides a basis for the development of functional materials based on graphene and metal nanoparticles, with potential catalytic and technological applications.

KEY WORDS: Silver nanoparticles, gold nanoparticles, graphene oxide, green synthesis.

Please cite this article as/Como citar este artículo: Del Real-Quiñonez, W.A., Lomelí-Rosales, D.A, Ramírez-González, D., Guevara-Martínez, S.J., Escutia-Gutiérrez, R., Del Río-Chávez, A. A., Zamudio-Ojeda A. (2025). Synthesis of gold and silver nanoparticles anchored in graphene oxide. *Revista Bio Ciencias*, 12, e1878. https://doi.org/10.15741/revbio.12.e1878

Article Info/Información del artículo
Received/Recibido: January 15th 2025.
Accepted/Aceptado: July 15th 2025.
Available on line/Publicado: August 11th 2025.

***Corresponding Author:**

Adalberto Zamudio-Ojeda. Departamento de Física, Centro Universitario de Ciencias Exactas e Ingenierías, Universidad de Guadalajara, Guadalajara, 44430, México. Teléfono: 52 (33) 1378 5900. ext. 27529. E-mail: adalberto.zojeda@academicos.udg.mx

Revista Bio ciencias
ISSN 2007-3380

RESUMEN

En este estudio se describe una serie de experimentos destinados al anclaje de nanopartículas de plata (AgNPs) y oro (AuNPs) sobre óxido de grafeno (GO). En una primera etapa, se realizó la síntesis de nanopartículas coloidales utilizando el método de Turkevich, empleando citrato de sodio como agente reductor y estabilizador. Posteriormente, se implementó el anclaje de las nanopartículas al GO, el cual fue sintetizado mediante el método modificado de Hummers, que involucra la oxidación de grafito utilizando permanganato de potasio ($KMnO_4$), nitrato de sodio ($NaNO_3$) y ácido sulfúrico (H_2SO_4). Para el anclaje, se desarrollaron dos metodologías: (1) mezcla de una solución de nanopartículas de Au o Ag con GO, y (2) síntesis in-situ de las nanopartículas en una solución de GO. Las muestras obtenidas fueron caracterizadas mediante espectroscopia ultravioleta-visible (UV-Vis), microscopía electrónica de barrido (SEM), microscopía electrónica de transmisión de alta resolución (HRTEM), dispersión dinámica de luz (DLS) y difracción de rayos X de polvos (XRD). Los resultados indican que ambos métodos son efectivos para el anclaje de nanopartículas, mostrando distribuciones homogéneas y buenas propiedades estructurales. Este estudio proporciona una base para el desarrollo de materiales funcionales basados en grafeno y nanopartículas magnéticas, con potencial en aplicaciones catalíticas y tecnológicas.

PALABRAS CLAVE: Nanopartículas de plata, nanopartículas de oro, óxido de grafeno, síntesis verde.

Introduction

At the end of the 20th century, a revolutionary scientific discipline known as Nanoscience emerged, focusing on the study of the unique properties that arise when materials have at least one of their dimensions at the nanometric scale (one billionth of a meter). These reduced dimensions impart atypical behaviors to materials compared to their macroscopic counterparts, including exceptional optical, electrical, and mechanical properties that position them as key tools for technological innovation (Xia *et al*., 2003). Although nanomaterials have intrinsically existed in nature, examples include the DNA double helix, which has a diameter of 2.5 nm (Zhao *et al*., 2014), the nanostructures coating the scales of butterfly wings from the Morpho genus (Zhang *et al*., 2015), and carbon formations in petroleum reservoirs (Galiakhmetova *et al*., 2024). Interestingly, the use of nanoparticles dates back to antiquity, as demonstrated by examples such as the Lycurgus Cup, renowned for its optical properties derived from AuNPs and AgNPs; Damascus swords, which contained carbon nanostructures that enhanced their strength and flexibility; and medieval stained glass, where metallic nanoparticles (MNPs) were used to generate vibrant colors. The

Revista Bio ciencias
ISSN 2007-3380

modern concept of Nanoscience was anticipated by Richard Feynman in his iconic 1959 lecture, Plenty of Room at the Bottom, where he envisioned the possibility of manipulating individual atoms and molecules to design materials with innovative properties (Feynman *et al*., 1960). Feynman emphasized that at such small scales, the laws of quantum mechanics prevail, opening the door to new physical phenomena and technological applications. However, it was not until the 1980s that Nanoscience emerged as a practical field, driven by the development of electron microscopes capable of visualizing, manipulating, and characterizing atomic-scale structures.

Today, Nanoscience is an interdisciplinary field involving scientists and engineers from disciplines such as physics, chemistry, biology, and electronics (Adams *et al*., 2016). Its applications range from energy and medicine to the development of electronic devices and self-evolving systems (Bensaude-Vincent *et al*., 2016). The ability to manipulate atoms and molecules enables the design of materials with enhanced or entirely new macroscopic properties. A representative example of these innovations is graphene, a carbon allotrope synthesized and stabilized for the first time in 2004 (Karthik *et al*., 2014). This material possesses exceptional properties, including high elasticity, thermal and electrical conductivity, making it an ideal candidate for applications in gas sensors, high-frequency electronics, fuel cells, and supercapacitors (Zhen *et al*., 2018). Additionally, graphene oxide (GO), derived from the oxidation of graphite, provides a functionalized platform for anchoring MNPs, enhancing the properties of the resulting hybrid materials (Smith *et al*., 2019).

Metal nanoparticles (MNPs), particularly silver and gold nanoparticles, have also revolutionized science and technology due to their unique nanoscale properties, such as changes in melting point, high surface area, and surface plasmon resonance, compared to macroscale structures of the same materials (Ghosh *et al*., 2007). These nanoparticles find applications in catalysis, medicine, biotechnology, energy, and electronic devices, positioning themselves as key tools in modern science (Coviello *et al*., 2022). This study explores the synthesis and anchoring of silver and gold nanoparticles onto GO, evaluating their structural and functional properties for potential applications in industry and research. It is important to highlight that the context in which nanoparticle anchoring onto the graphene surface is defined refers to the process of binding or immobilizing MNPs on its surface due to physical interactions, such as electrostatic forces, or chemical interactions, through the formation of covalent bonds between GO functional groups and MNPs (Goncalves *et al*., 2009).

In recent years, Nanoscience has developed various methods for nanoparticle synthesis, which can be broadly categorized into chemical and physical methods. The former is typically based on the reduction of metal salts, while the latter involves the evaporation of macroscopic materials. One commonly used physical method is laser ablation, which involves directing a laser beam to remove material from a solid surface (Lin *et al*., 2015). Another method is electric arc discharge, in which material is vaporized from a cathode (Tsai *et al*., 2013). Although physical methods such as laser ablation and cathodic arc deposition can produce high-purity nanostructures, their main drawback is the requirement for specialized equipment, which can cost from tens of thousands to millions of dollars. In contrast, chemical methods rely on the use of metal salts, where metal atoms in an oxidation state different from zero must be reduced in a medium. Various solvents

Revista Bio ciencias
ISSN 2007-3380

and reducing agents (e.g., hydrides or hydrazines) are employed, along with a stabilizer (Li *et al*., 2021). This approach is known as the bottom-up method, as it starts with individual atoms that are systematically assembled to form the nanostructure. The advantage of this particle-generation method is that it does not require expensive equipment, making it highly convenient for implementation in laboratories.

Metallic nanoparticles (MNPs), known for their high electrical and thermal conductivity, chemical stability, and surface plasmon resonance, offer a wide range of applications, from sensors and catalysis to controlled drug delivery systems and antimicrobial therapies (Shnoudeh *et al*., 2019). Meanwhile, GO, derived from graphene through oxidation processes, provides an ideal functionalized platform due to its high surface area, mechanical flexibility, and oxygenated functional groups. The combination of AuNPs or AgNPs with GO generates hybrid materials that maximize the individual properties of each component, creating synergies that enhance their applicability (Majumder *et al*., 2022). This anchoring process can occur through physical interactions, such as electrostatic bonds, or chemical interactions, such as covalent bonding between GO functional groups and MNPs (Narayan *et al*., 2024). Additionally, *in-situ* synthesis, where nanoparticles are generated directly in the presence of GO, allows precise control over nanoparticle distribution and size, optimizing the resulting material's properties (Badoni *et al*., 2024).

Hybrid AuNPs/AgNPs-GO materials have demonstrated significant potential in various fields, including the energy sector—directly impacting the development of solar cells and supercapacitors; catalysis—enhancing chemical reactions with high efficiency; medicine—with applications in antimicrobial therapies and biomedical imaging (Ray *et al*., 2024); and electronics—through the development of advanced sensors and flexible devices (Darabdhara *et al*., 2019). These applications underscore the scientific and technological relevance of hybrid nanomaterials, as well as their role in designing sustainable and highly functional solutions (Yin *et al*., 2015). The present study explores the synthesis and characterization of AuNPs and AgNPs anchored onto GO, emphasizing anchoring methods and the properties obtained in relation to their applicability in industry and research (Yuan *et al*., 2018). This approach significantly contributes to advancing knowledge in Nanoscience and functional materials (Pang *et al*., 2023).

Material and Methods

Material

The reactions were carried out using high-purity reagents and solvents, which were purchased from Sigma-Aldrich and Merck. The water used for nanoparticle synthesis was bidistilled and deionized. The reagents used, Tetrachloroauric Acid ($HAuCl_4 \cdot 3H_2O$) and Silver Nitrate ($AgNO_3$), were kept under an inert atmosphere in a glove box to prevent hydration.

Characterization Techniques

The obtained samples were characterized using UV-Vis spectroscopy with a Thermo Scientific

Revista Bio ciencias
ISSN 2007-3380

Genesis 10S UV-Vis spectrophotometer. Scanning electron microscopy (SEM) images were obtained using a TESCAN MIRA 3MLU microscope, operating at 20 kV. High-resolution transmission electron microscopy (HRTEM) images were obtained using an FEI TECNAI F30 STWIN G2 microscope at 300 kV. For sample preparation, copper grids (200 mesh) were used, onto which a diluted drop of the material to be analyzed was deposited. For X-ray diffraction (XRD) analysis, an Empyrean diffractometer with Cu-Kα radiation (λ = 1.5406 Å) was used, with a current intensity of 20 mA, a voltage of 30 kV, and a scanning speed of 0.02 degrees/second. The dynamic light scattering (DLS) technique was employed to determine the average particle size using a Zetasizer Nano S90 Malvern.

Synthesis of Graphene Oxide (GO)

GO was synthesized using a modified Hummers method, which involves adding graphite flakes and immersing them in acid, followed by the addition of $KMnO_4$. Once all materials were mixed, a turbid brown coloration was obtained, and the substance was gradually diluted by carefully adding water until an amber color was achieved. Hydrogen peroxide (H_2O_2) was then added to complete the reaction, followed by sonication to separate the GO sheets.

Synthesis of Metallic Nanoparticles (MNPs)

The synthesis of AuNPS and AgNPs was carried out following the methodology developed by Turkevich, adding a reflux system that prevented solvent evaporation during the synthesis process. The methodology used in each process is described below.

Synthesis of Silver Nanoparticles (AgNPs)

$AgNO_3$ was used as the silver source, and sodium citrate served as both the reducing and stabilizing agent. Using a reflux system, 50 mL of distilled water was added to a flask, followed by 15 mL of a previously prepared sodium citrate solution (1.108 mM in water) under heating at 100°C and stirring at 1000 rpm. Then, 9.6 mg of silver nitrate was added. The reaction mixture was maintained under constant stirring and temperature for 45 minutes until a color change from transparent to yellow was observed.

Synthesis of Gold Nanoparticles (AuNPs)

The synthesis was carried out using $HAuCl_4 \cdot 3H_2O$ as the gold source and sodium citrate as the reducing and stabilizing agent. The same experimental setup as for AgNP synthesis was used. A reflux system was employed, in which 20 mL of distilled water and 1 mL of sodium citrate solution (1.108 mM) were added to the flask. The system was heated to 100 °C and stirred at 1000 rpm. Once this temperature was reached, 0.45 mL of a 0.218 mM $HAuCl_4 \cdot 3H_2O$ solution in water was added. The reaction was maintained under the same temperature and stirring conditions for 40 minutes until a color change from transparent to cherry red was observed.

Revista Bio ciencias
ISSN 2007-3380

Two-Step Method for Anchoring MNPs onto GO

In this method, colloidal Ag and Au nanoparticles were synthesized as previously described. Separately, 1 mL of GO (0.2 mg/mL concentration) was added to each nanoparticle solution, and the mixture was stirred at 1000 rpm and room temperature (25 °C) for 15 minutes. After completing the process, samples were collected for characterization.

One-Step *in situ* Method for Anchoring MNPs onto GO

Two reflux systems (one for silver and one for gold) were employed, using the same concentrations of metal salts and citrate as in the metallic nanoparticle synthesis. The reagent addition sequence was as follows: a) 20 mL of water, b) the corresponding amount of metal salt (9.6 mg $AgNO_3$ or 0.45 mL of a 0.218 mM $HAuCl_4$ solution), c) 1 mL of GO (0.2 mg/mL concentration).

The system's heating parameters were then adjusted to 100°C and 1000 rpm. Once the synthesis conditions stabilized, the appropriate amount of citrate solution was added to each flask (15 mL for Ag and 1 mL of a 1.108 mM sodium citrate solution for Au). Both reactions were maintained under these conditions for 40 minutes (as in the synthesis of their respective colloidal nanoparticles). After completing the process, samples were collected for characterization.

Results and discussion

Characterization of Graphite by SEM and XRD

For the OG synthesis, graphite flake powder was used and analyzed in SEM. The sample preparation consisted of sticking a double-layer tape on an aluminum pin, where graphite flake powder was placed on the top layer of the tape. Once the sample was prepared, it was entered into SEM. The voltage used to analyze the sample was 30 KV. The results showed structures with average dimensions of 1 mm^2 (Figure 1a) and a thickness of 20 µm (Figure 1b). This thickness is equivalent to about 60,000 stacked graphene layers. The calculation was made by considering the size of a carbon atom is 0.070 nm, the separation between the layers, and dividing this result by the thickness of the graphite flake. Figure 1a shows a large concentration of graphite plates with irregular shapes and rough surfaces.

Revista Bio ciencias
ISSN 2007-3380

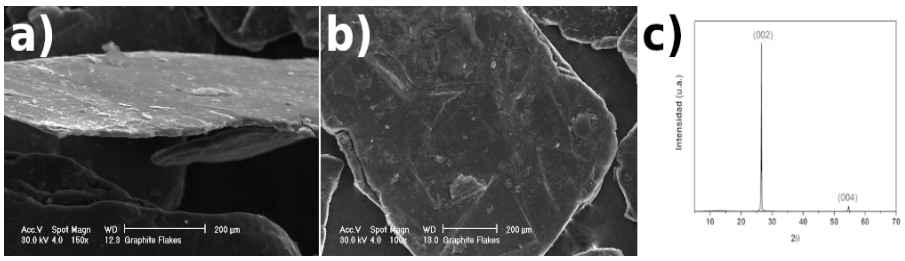

Figure 1. SEM images obtained at a voltage of 30 kV.

a) Graphite flakes at 35 magnifications with an average area of 1 mm², b) Thickness of a graphite flake (20 µm) at 500 magnifications; c) X-ray diffractogram of a graphite flake.

In the x-ray diffractogram (Figure 1c) it is observed that the graphite is crystalline and has a maximum peak at 2θ = 26.1°, which corresponds to a direction of the crystalline plane in [002], with an interplanar distance of 0.34 nm calculated with Bragg's law (Ramírez-Gonzalez *et al*., 2020).

Characterization of the GO by SEM, HRTEM, and XRD

A GO sample was characterized by SEM. The voltage used for the analysis was 20 KV, Figure 2a shows that the surface of the GO is not uniform, it presents a rough morphology.

The HRTEM characterization images are presented in Figure 2b, where the presence of graphene oxide sheets (GO) is observed. The presence of graphite oxide is ruled out, since the electron beam transmittance is similar to that reported by Marcelo M. Viana and co-workers (Viana *et al*., 2015). In this, it can be observed that the sheets have a rough surface and a color change can be seen on the surface of the material, which indicates that the darker part has a greater number of layers than the lighter part, this because in the areas of higher density of material the electron adsorption increases. Figure 2c, shows the XRD of the GO, it is observed that it is crystalline and has a maximum peak at 2θ = 13°, which corresponds to a direction of the crystalline plane in [002], with an interplanar distance of 0.72 nm calculated using Bragg's law (Ramírez-Gonzalez *et al*., 2020). There is also a shift with respect to the results of graphite, which shows a maximum peak at 2θ = 26.1°, which indicates a change in the crystalline structure.

Revista Bio ciencias
ISSN 2007-3380

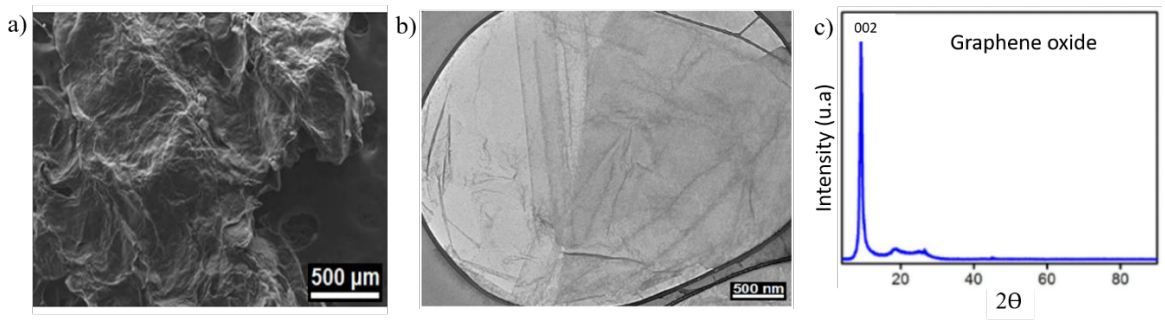

Figure 2. a) SEM image obtained at 20 kV, GO sheet; b) HRTEM obtained at 49000 amplifications at 100 KV, GO sheets; c) X-ray diffractogram for GO sheets.

Synthesis of AgNPs

The resulting AgNPs present a yellow amber color, which changes to a cloudy amber depending on the amount and/or size of the particles contained in the system, as can be seen in Figure 3a. This is due to the exposure time of the mixture at a given temperature, depending on the aging of the system the particles grow in size and agglomerate. The samples labeled Ag 1, Ag 2, and Ag 3, were synthesized at different reaction times at 30, 33, and 35 minutes respectively. When the samples were analyzed by UV-Vis, the spectra in Figure 3b were obtained, showing the maximum absorption peaks for Ag 1, Ag 2, and Ag 3 samples with wavelengths of 425, 431, and 433 nm, respectively. Figure 3c, shows the HRTEM characterization, analyzed on a 200 mesh copper grid, at a voltage of 100 KeV. The images obtained show the presence of AgNPs, which present different undefined geometrical structures concentrated in a small cluster, showing average sizes between 30-50 nm. Using the DLS technique, an average particle size of 31.39 nm was found.

Revista Bio ciencias
ISSN 2007-3380

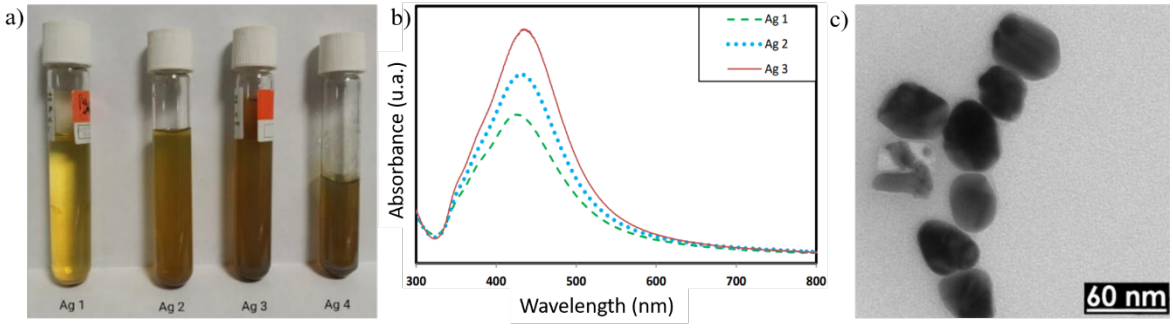

Figure 3. a) AgNPs samples, which show a yellow to amber color. The difference in coloration depends on the concentration and size of the particles; b) UV-Vis graphs for the extracted AgNPs samples; c) HRTEM at 100 KV of AgNPs clusters where the particles show diameters of 30 to 80 nm at 623,000 magnifications.

Synthesis of AuNPs

The AuNPs exhibited a cherry-pink coloration, which remained unchanged across the different extracted samples (Figure 4a). The samples designated as Au 1, Au 2, and Au 3 correspond to extraction times of 30, 35, and 40 minutes, respectively. The obtained samples were analyzed using UV-Vis spectroscopy, with the results shown in Figure 4b. A maximum peak was observed at 537 nm for the Au1 sample, 535 nm for the Au2 sample, and 536 nm for the Au3 sample. For HRTEM characterization, the sample was prepared using a 200-mesh grid at an accelerating voltage of 100 keV. Figure 4c illustrates the formation of gold colloids in our synthesis. The particles present in our samples have diameters ranging from 15 to 25 nm with irregular morphologies. Using the DLS technique, the average particle size was determined to be 18.8 nm.

Revista Bio ciencias
ISSN 2007-3380

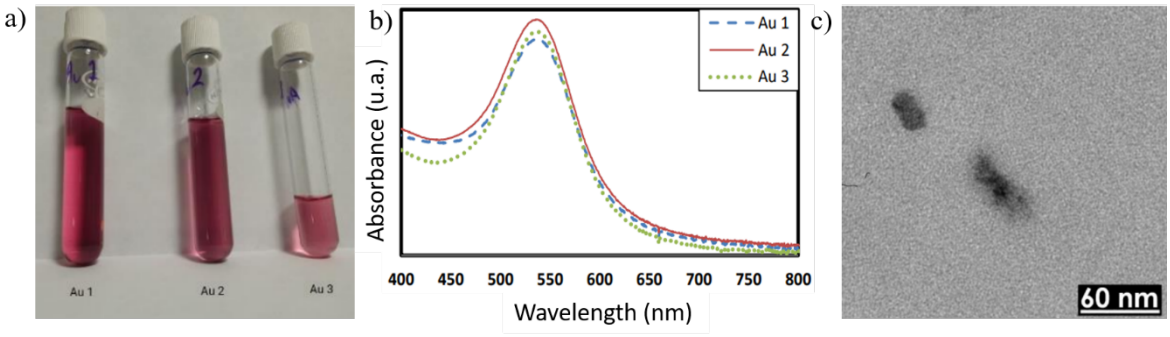

Figure 4. a) AuNPs show cherry coloration at different reaction times; b) UV-Vis of AuNPs; c) HRTEM at 100 KV and 623,000 amplifications shows the formation of AuNPs with diameters of 20 to 25 nm.

In Situ Anchoring Method with AgNPs

The sample was characterized using SEM to observe the distribution of metallic particles on the GO sheets (Figure 5a). By employing the backscattered electron (BSE) detector, atomic weight contrast was obtained, where light atoms such as carbon appear gray or dark, while heavier materials (in this case, silver) appear brighter. Due to the contrast between elements, it is evident that the AgNPs exhibit an almost homogeneous distribution along the GO surface, with some brighter areas where larger particles or higher concentrations of particles are present. Variations in grayscale indicate that the GO surface is not uniform and possesses roughness throughout. These images reveal significant changes that occur when synthesizing MNPs in the presence of GO (*in situ* method) compared to the morphologies adopted by nanoparticles in the absence of GO, as shown in Figure 3c. In the GO presence, the observed morphologies include spheres, rods, wires, cylinders, triangles, regular and irregular rectangles, pentagons, hexagons, heptagons, octagons, etc. Additionally, a wide range of particle sizes is observed, including particles with diameters of 5–100 nm, nanorods with lengths of 50–800 nm, and diameters ranging from 18 to 45 nm (Figures 5b and 5c).

Revista Bio ciencias
ISSN 2007-3380

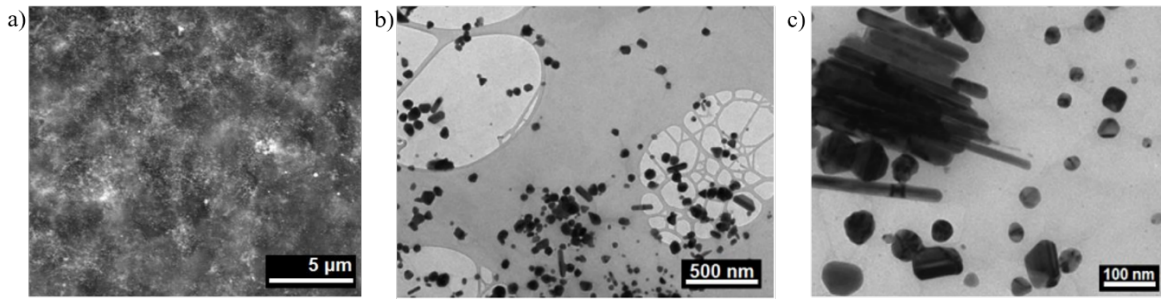

Figure 5. a) SEM at 5,000 magnifications and 20 KV, dispersion of AgNPs (white dots) on the surface of the GO (dark surface); b) HRTEM at 156,000 magnifications and 105 KV. Agglomeration of silver cylinders, along with other geometric figures; c) HRTEM at 117,000 magnifications and 105 KV, showing a greater difference in diameters between them, in addition to other rhomboids.

Two-Step Anchoring Method with AgNPs

Figure 6a presents an HRTEM image obtained at an accelerating voltage of 100 keV, showing a GO sheet with AgNPs. The sheet exhibits different shades of gray, indicating regions with a greater number of layers as well as surface roughness. The nanoparticles are not uniformly distributed; they are predominantly located at the edges of the GO sheet. Figure 6b displays clusters of particles in the central region of the GO sheet, exhibiting a wide range of sizes from 5 nm to 35 nm, with most nanoparticles adopting spherical shapes and some appearing as amorphous structures.

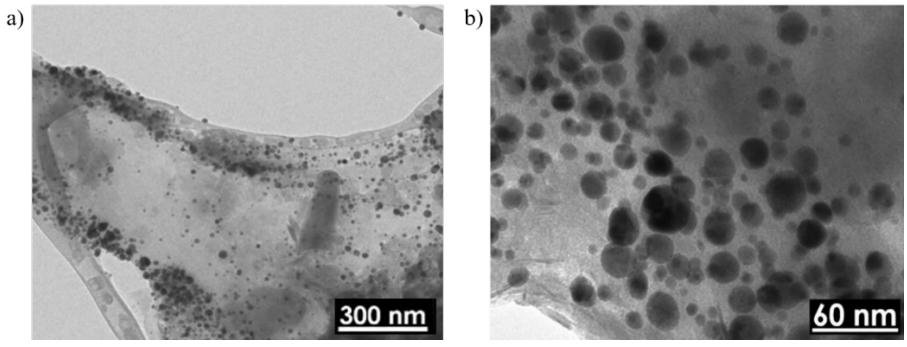

Figure 6. a) HRTEM at 94,200 magnifications and 100 KV shows the formation of silver metallic spheres on the surface of the GO with diameters of 5-35 nm; b) Magnification at 623,000 magnifications shows more clearly the silver particles in the GO.

Revista Bio ciencias
ISSN 2007-3380

In Situ Anchoring Method with AuNPs

SEM characterization reveals the dispersion of particles on GO. In Figure 7a, BSE imaging provides atomic weight contrast, where the grayscale range is defined by particle weight, with heavier particles appearing white and lighter ones appearing black. In this case, gold is heavier than carbon, resulting in an almost homogeneous distribution of white spots across the carbon surface. Larger white spots may correspond to larger particles or aggregates of medium-sized particles. Variations in grayscale may be due to irregularities across the GO surface. HRTEM characterization, conducted on a copper 200-mesh grid at an accelerating voltage of 100 keV, reveals in Figure 7b the predominant presence of well-defined spherical structures with diameters ranging from 10 to 30 nm. Using the DLS technique, the average particle size was determined to be 31.39 nm. Other irregularly shaped structures such as triangles and squares, with dimensions similar to those of the spheres, were also observed. Additionally, larger gold aggregates with amorphous morphologies were found, measuring between 50 and 100 nm. In these cases, the graphene sheets appear nearly transparent, indicating minimal imperfections such as surface roughness and a nearly uniform density.

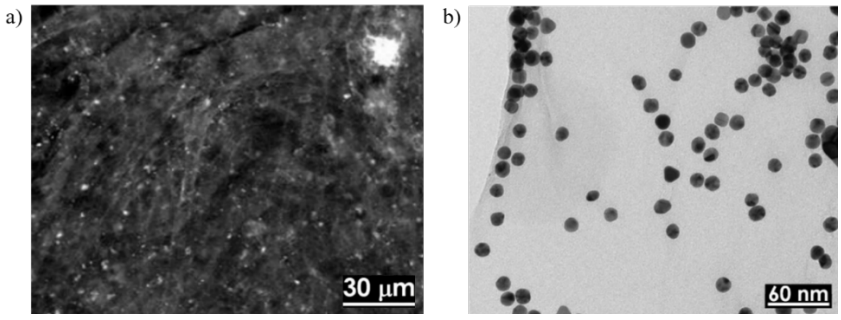

Figure 7. a) SEM at 1,000 magnifications and 20 KV, the homogeneous distribution of metallic particles on the surface of the GO can be observed; b) HRTEM at 467,000 magnifications and 105 KV spherical particles and formation of triangles and squares.

Two-Step Anchoring Method with AuNPs

HRTEM characterization (Figure 8a) shows the anchoring of AuNPs on the GO surface. A high concentration of semi-spherical particles of varying sizes, as well as amorphous structures likely resulting from the fusion of spheres, is observed. Additionally, large gold clusters exceeding 150 nm in diameter are present. The spherical and amorphous structures range in size from 5 nm to 50 nm (Figure 8b). When examining the GO sheet on which the nanoparticles are deposited, numerous surface defects are evident. However, unlike other samples, the sheet exhibits an almost homogeneous gray contrast, indicating a relatively uniform thickness in this case.

Revista Bio ciencias
ISSN 2007-3380

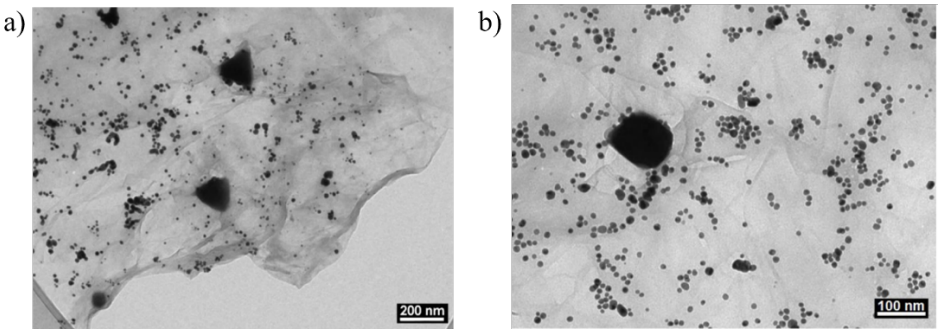

Figure 8. a) HRTEM at 93,400 magnifications and 100 KV, gold particles anchored to the graphene surface can be observed; b) magnification at 195,000 and 105 KV, sizes and shapes that can vary from 5 to 150 nm can be observed.

Conclusions

The synthesis of metallic nanoparticles (MNPs) was successfully carried out, yielding spheroidal particles with distinctive structural properties. Silver nanoparticles (AgNPs) were found to be metastable, with an average size ranging from 30 to 50 nm, ensuring their dispersion in colloidal media. On the other hand, gold nanoparticles (AuNPs) exhibited remarkable post-synthesis stability, maintaining uniform sizes between 15 and 25 nm without significant variations. Graphene oxide (GO) played a crucial role as a substrate, controlling the stability and distribution of the nanoparticles, a behavior similar to that reported by D. Ramírez and colleagues, who used nitrogen-doped graphene sheets to anchor AgNPs (Ramírez-Gonzalez *et al*., 2020).

The results demonstrated that incorporating GO before the synthesis (*in situ* method) enabled more efficient nucleation, significantly reducing reaction times and ensuring uniform anchoring onto the graphene structure. This behavior suggests that the oxygenated groups of GO promote nanoparticle formation by acting as nucleation sites, which aligns with previous studies. Additionally, the morphology of the obtained nanoparticles was variable, which could be attributed to the influence of the heterogeneous nucleation and growth process. Findings by Xiu-Zhi Tang and colleagues on the synthesis of AgNPs on GO, compared to those synthesized in the presence of reduced graphene, showed that in the former case, the nanoparticles tended to better coat the GO surfaces due to the polar interaction of silver with the polar sites (Xiu-Zhi *et al*., 2013). This finding is consistent with reports by G. Gonçalves and colleagues, who stated that the presence of oxygen sites serves as nucleation points for nanoparticle growth (Darabdhara *et al*., 2019).

It is noteworthy that nanoparticle morphology can be controlled using different stabilizing agents or templates (Restrepo *et al*., 2021). However, our results reveal diverse morphologies, possibly due to the fact that during the nucleation process, particles grow from a seed, allowing

Revista Bio ciencias
ISSN 2007-3380

heterogeneous growth of the nanostructure. Taken together, these findings highlight the importance of GO as a versatile functional support that not only stabilizes MNPs but also helps preserve their physicochemical properties, thereby expanding their potential applications in the biomedical and environmental fields.

Author Contributions

Conceptualization: W.A.R-Q., D.R-G., R.E-G., S.J.G-M., D.A.L-R., A.A.R-C., A.Z-O.; Writing—original draft preparation: S.J.G-M., D.A.L-R., R.E-G., and A.Z-O.; Writing—review and editing: W.A.R-Q., D.R-G., R.E-G., S.J.G-M., D.A.L-R.; Visualization: A.Z-O. and S.J.G-M.; Project administration: S.J.G-M. and A.Z-O.; Supervision: W.A.R-Q., D.R-G., R.E-G., S.J.G-M., D.A.L-R., A.A.R-C., A.Z-O.

All authors have read and approved the published version of the manuscript.

Funding

This research received no external funding.

Ethical Statements

Not applicable.

Informed Consent Statement

Not applicable.

Acknowledgments

Special thanks to the Centro Universitario de Ciencias Exactas e Ingenierías of the Universidad de Guadalajara (UdG) for their support with the characterization techniques used in this project.

Conflict of Interest

The authors declare no conflict of interest.

References

Adams, F. C., & Barbante, C. (2013). Nanoscience, nanotechnology and spectrometry. Spectrochimica Acta Part B: Atomic Spectroscopy, 86, 3-13. https://doi.org/10.1016/j.sab.2013.04.008

Badoni, A., & Prakash, J. (2024). Noble metal nanoparticles and graphene oxide based hybrid nanostructures for antibacterial applications: Recent advances, synergistic antibacterial activities, and mechanistic approaches. *Micro and Nano Engineering*, *22*, 100239. https://doi.org/10.1016/j.mne.2024.100239

Bensaude-Vincent, B. (2016). Building multidisciplinary research fields: The cases of materials science, nanotechnology and synthetic biology. In *The Local Configuration of New Research Fields: On Regional and National Diversity* (pp. 45-60). Cham: Springer International Publishing. https://doi.org/10.1007/978-3-319-22683-5_3

Coviello, V., Forrer, D., & Amendola, V. (2022). Recent developments in plasmonic alloy nanoparticles: synthesis, modelling, properties and applications. *ChemPhysChem*, *23*(21), e202200136. https://doi.org/10.1002/cphc.202200136

Darabdhara, G., Das, M. R., Singh, S. P., Rengan, A. K., Szunerits, S., & Boukherroub, R. (2019). Ag and Au nanoparticles/reduced graphene oxide composite materials: synthesis and application in diagnostics and therapeutics. *Advances in colloid and interface science*, *271*, 101991. https://doi.org/10.1016/j.cis.2019.101991

Feynmann, R. P. (1960). There's plenty of room at the bottom. *Eng. Sci*, *23*(5), 22-36. https://www.zyvex.com/nanotech/feynman.html

Galiakhmetova, L. K., Kayumov, A. A., Katnov, V. E., Khelkhal, M. A., Mukhamatdinova, R. E., Trubitsina, S. A., ... & Vakhin, A. V. (2024). Thermal steam treatment effect of metallic sodium nanoparticles for high-carbon, low permeability Domanic rocks. *Geoenergy Science and Engineering*, 240, 213038. https://doi.org/10.1016/j.geoen.2024.213038

Ghosh, S. K., & Pal, T. (2007). Interparticle coupling effect on the surface plasmon resonance of gold nanoparticles: from theory to applications. *Chemical reviews*, *107*(11), 4797-4862. https://doi.org/10.1021/cr0680282

Goncalves, G., Marques, P. A., Granadeiro, C. M., Nogueira, H. I., Singh, M. K., & Gracio, J. (2009). Surface modification of graphene nanosheets with gold nanoparticles: the role of oxygen moieties at graphene surface on gold nucleation and growth. *Chemistry of Materials*, 21(20), 4796-4802. https://doi.org/10.1021/cm901052s

Karthik, P. S., Himaja, A. L., & Singh, S. P. (2014). Carbon-allotropes: synthesis methods, applications and future perspectives. *Carbon letters*, *15*(4), 219-237. https://doi.org/10.5714/CL.2014.15.4.219

Lin, T. N., Chih, K. H., Yuan, C. T., Shen, J. L., Lin, C. A. J., & Liu, W. R. (2015). Laser-ablation production of graphene oxide nanostructures: from ribbons to quantum dots. *Nanoscale*, *7*(6), 2708-2715. https://doi.org/10.1039/C4NR05737F

Li, X., & Binnemans, K. (2021). Oxidative dissolution of metals in organic solvents. *Chemical Reviews*, *121*(8), 4506-4530. https://doi.org/10.1021/acs.chemrev.0c00917

Majumder, P., & Gangopadhyay, R. (2022). Evolution of graphene oxide (GO)-based nanohybrid

Revista Bio ciencias
ISSN 2007-3380

materials with diverse compositions: an overview. *RSC advances*, 12(9), 5686-5719. https://doi.org/10.1039/D1RA06731A

Narayan, J., & Bezborah, K. (2024). Recent advances in the functionalization, substitutional doping and applications of graphene/graphene composite nanomaterials. *RSC advances*, 14(19), 13413-13444. https://doi.org/10.1039/D3RA07072G

Pang, J., Peng, S., Hou, C., Zhao, H., Fan, Y., Ye, C., ... & Cuniberti, G. (2023). Applications of graphene in five senses, nervous system, and artificial muscles. *ACS sensors*, 8(2), 482-514. https://doi.org/10.1021/acssensors.2c02790

Ramírez-Gonzalez, D., Cruz-Rivera, J. de J., Tiznado, H., Rodriguez, A. G., Guillen-Escamilla, I., & Zamudio-Ojeda, A. (2020). Caffeine as a source for nitrogen doped graphene, and its functionalization with silver nanowires *in-situ*. *Advances in Nano Research*, 9(1), 25–32. https://doi.org/10.12989/ANR.2020.9.1.025

Ray, S. C., Mishra, D. K., & Pong, W. F. (2024). Optimization of Magnetic Behaviors of Au-NP-Decorated MWCNTs and Reduced Graphene Oxide for Biomedical Applications. *ACS omega*, 9(38), 40067-40074. https://doi.org/10.1021/acsomega.4c05962

Restrepo, C. V., & Villa, C. C. (2021). Synthesis of silver nanoparticles, influence of capping agents, and dependence on size and shape: A review. *Environmental Nanotechnology, Monitoring & Management*, *15*, 100428. https://doi.org/10.1016/j.enmm.2021.100428

Shnoudeh, A. J., Hamad, I., Abdo, R. W., Qadumii, L., Jaber, A. Y., Surchi, H. S., & Alkelany, S. Z. (2019). Synthesis, characterization, and applications of metal nanoparticles. *In Biomaterials and bionanotechnology* (pp. 527-612). Academic Press. https://doi.org/10.1016/B978-0-12-814427-5.00015-9

Smith, A. T., LaChance, A. M., Zeng, S., Liu, B., & Sun, L. (2019). Synthesis, properties, and applications of graphene oxide/reduced graphene oxide and their nanocomposites. *Nano Materials Science*, *1*(1), 31-47. https://doi.org/10.1016/j.nanoms.2019.02.004

Tang, X. Z., Li, X., Cao, Z., Yang, J., Wang, H., Pu, X., & Yu, Z. Z. (2013). Synthesis of graphene decorated with silver nanoparticles by simultaneous reduction of graphene oxide and silver ions with glucose. *Carbon*, 59, 93-99. https://doi.org/10.1016/j.carbon.2013.02.058

Tsai, W. Y., Lin, R., Murali, S., Zhang, L. L., McDonough, J. K., Ruoff, R. S., ... & Simon, P. (2013). Outstanding performance of activated graphene based supercapacitors in ionic liquid electrolyte from− 50 to 80 C. *Nano Energy*, *2*(3), 403-411. https://doi.org/10.1016/j.nanoen.2012.11.006

Viana, M. M., Lima, M. C., Forsythe, J. C., Gangoli, V. S., Cho, M., Cheng, Y., ... & Caliman, V. (2015). Facile graphene oxide preparation by microwave-assisted acid method. *Journal of the Brazilian Chemical Society*, 26(5), 978-984. https://doi.org/10.5935/0103-5053.20150061

Xia, Y., Yang, P., Sun, Y., Wu, Y., Mayers, B., Gates, B., ... & Yan, H. (2003). One-dimensional nanostructures: synthesis, characterization, and applications. *Advanced materials*, *15*(5), 353-389. https://doi.org/10.1002/adma.200390087

Yin, P. T., Shah, S., Chhowalla, M., & Lee, K. B. (2015). Design, synthesis, and characterization of graphene–nanoparticle hybrid materials for bioapplications. *Chemical reviews*, *115*(7), 2483-2531. https://doi.org/10.1021/cr500537t

Yuan, Z., Xiao, X., Li, J., Zhao, Z., Yu, D., & Li, Q. (2018). Self-assembled graphene-based architectures and their applications. *Advanced Science*, 5(2), 1700626. https://doi.org/10.1002/advs.201700626

Revista Bio ciencias
ISSN 2007-3380

Zhao, M. Q., Zhang, Q., Tian, G. L., & Wei, F. (2014). Emerging double helical nanostructures. *Nanoscale*, *6*(16), 9339-9354. https://doi.org/10.1039/C4NR00271G

Zhang, D., Zhang, W., Gu, J., Fan, T., Liu, Q., Su, H., & Zhu, S. (2015). Inspiration from butterfly and moth wing scales: Characterization, modeling, and fabrication. *Progress in Materials Science*, *68*, 67-96. https://doi.org/10.1016/j.pmatsci.2014.10.003

Zhen, Z., & Zhu, H. (2018). Structure and properties of graphene. In Graphene (pp. 1-12). Academic Press. https://doi.org/10.1016/B978-0-12-812651-6.00001-X